Island Shape Instabilities and Surfactant-Like Effects in the Growth of InGaAs/GaAs Quantum Dots

R. Leon*, C. Lobo#, X. Z. Liao+, J. Zou+, D. J. H. Cockayne+ and S. Fafard**

**Jet Propulsion Laboratory, California Institute Of Technology, 4800 Oak Grove Drive, Pasadena, CA 91109-8099*
 # Research School of Physical Sciences, Australian National University, Canberra, ACT 0200, Australia
+ Australian Key Centre for Microscopy and Microanalysis, The University of Sydney, Sydney, NSW 2006, Australia
*** Institute for Microstructural Sciences, National Research Council, Ottawa, Ontario, Canada K1A 0R6*

ABSTRACT

InGaAs/GaAs island formation during **vapor phase epitaxy** showed diverging behaviors when varying group V partial pressures (PP). Differences include changes in critical thicknesses for the onset of the Stranski-Krastanow (S-K) transformation, surface coverages, ratios between coherent and incoherent islands, and dissimilar morphologies upon annealing. These results show that slightly different values for the 2-D to 3-D transition can also be obtained in InGaAs/GaAs depending on AsH_3 PP. Photoluminescence spectroscopy of capped islands showed that the wetting layer thickness does not change beyond the onset of the S-K transformation for conditions producing stable islands. Annealing experiments done at high AsH_3 PP show Ostwald ripening, but we also observe that small, high density, lens-shaped islands are unaffected by prolonged annealing and do not ripen when an "optimum" low AsH_3 PP are used during the island growth and in-situ annealing. The later experiments show that small lens shaped islands can be found in equilibrium if InGaAs surface energies are minimized. These findings lead to the conclusion that AsH_3 can raise surface energies acting as an impurity-free "morphactant" in InGaAs growth.

self-organized growth
heteroepitaxy
critical thickeners

INTRODUCTION

The importance of Stranski-Krastanow (S-K) coherent island formation as a mechanism for strain relaxation has been established in both Ge/Si [1] and InAs/GaAs [2,3] heteroepitaxy. Interest in S-K growth has been re-kindled by the first reports of these strained islands to make defect-free, self-assembled, InGaAs/GaAs semiconductor quantum dots [4-6]. Since then, a large number of studies have focussed on strain relaxation by island formation. An improved understanding of the varying and often competing mechanisms that result in different morphologies during island nucleation will have a decisive effect on the successful utilization of these islands in semiconductor zero-dimensional (0-D) structures. Island shapes, aspect ratios, morphologies, and coherence/incoherence all play a role into the electronic/optic/magnetic properties of self-forming semiconductor quantum dots.

Recent reports show ripening behavior during island formation in Ge/Si heteroepitaxy. An in-situ study of the evolution of growth in Ge/Si to the stable dome shaped configuration found an optimum range in uniformity [7], desirable for device applications. Other reports show the coexistence of different types of islands [8] and a shape transition from small pyramid shaped islands to domes upon annealing [9]. In InGaAs/GaAs QD formation, ripening has also been observed upon annealing, which is partially suppressed by steps in miscut substrates [10]. The observation of ripening in S-K islands suggests that the small islands used for QDs might be unstable or metastable, with obvious disadvantages for optoelectronic applications of these island-based devices. Determining if stable islands can be achieved is thus of considerable practical and fundamental interest.

Several studies using surfactants in the growth of Ge/Si have produced striking results, from the total suppression of the S-K transformation [11,12], to different critical

thicknesses for such transformation [13] and different island shapes [14] with facetting from lower energy surfaces. No equivalent studies exist for the InGaAs/GaAs system, however it is plausible that such surfactant induced effects might explain the present controversy in the different shapes reported for InGaAs and InAs islands.

Kinetic suppression of island formation has been observed for low adatom diffusion lengths, thus accomplishing 2-D growth of InGaAs films at low temperature [15]. Here we report on a suppression of the S-K transformation, but rather than kinetically limited, our results can be better explained by an offset of the energetics driving the islanding transition. Annealing experiments done at high AsH_3 partial pressures concur with the observation of Ostwald ripening, but we also observed small, numerous lens shaped island after prolonged annealing. These results are important to establish the long-term stability of devices based on self-forming semiconductor quantum dots.

EXPERIMENT

InGaAs/GaAs structures were grown by metalorganic chemical vapor deposition (MOCVD). Growth conditions have been reported elsewhere for growth of InGaAs QDs on GaAs (100) [16], using graded growth rates to study the structural evolution of InGaAs S-K formation [17] and to achieve varying island densities in QD growth by varying group V partial pressures [18]. After island growth, the uncapped structures used in this study were cooled to room temperature in the growth chamber, maintaining the Arsine partial pressures to 400°C. Force microscopy (FM) with standard etched silicon nitride tips gave statistical information on island sizes and areal densities. Plan view and cross section transmission electron microscopy (TEM) and scanning electron microscopy (SEM) were also used for some of the samples. Low (77 K)

temperature photoluminescence (PL) spectra were obtained using the 532 nm continuous-wave output of a diode-pumped Nd:YVO_4 for excitation. The signal was dispersed with a single grating (0.67 m) monochromator, and collected using a cooled Ge detector and lock-in techniques.

RESULTS

In Figure 1, the fractional surface coverage from nanometer size InGaAs islands is examined. Growths were done under identical conditions except for the Arsine partial pressures. Figure 1 shows the statistical analysis of 2 types of islands: small coherent islands that are used in quantum dot applications, and larger islands that are found to coexist with the QDs in different ratios, which are seen to depend critically on growth conditions. Figure 2 (a) shows a plan view TEM micrograph illustrating the coexistence of both types of islands. The arrows in the figure point to the large incoherent islands. TEM observation of different samples under various growth conditions confirm that the larger faceted islands are incoherent, containing dislocations within. The solid diamonds and circles in figure 1 show the average diameters and the fractional surface coverages from these large islands, indicating that their density and sizes are dependent on arsine flow. The fractional coverage for the small islands (QDs) is significantly higher for an "optimal" value in Arsine pp, changing from a maximum of 25% for values of AsH_3 pp near 10^{-6} to only 5% for pp near 10^{-5}. Surface densities and dimensions for large islands are higher for the conditions that promote low coverage by small islands indicating opposing trends between small and large island coverages.

A different type of experiment is presented in figure 3. Depositions using graded growth rates were performed for different values of Arsine partial pressures. Gradients in quantum dot density can be produced by MOCVD by varying the carrier gas (H_2) flow. Numerical

simulations of concentration profiles and QW emission energy variations in capped samples were used to obtain an equivalent scale in monolayers (MLs) deposition for this technique [17]. This allowed determination of the 2-D to 3-D transitions for $In_{0.6}Ga_{0.4}As/GaAs$ in a similar fashion as reported by Leonard [19] and Kobayashi [20] for InAs/GaAs. Our experiments demonstrate a similar exponential behavior in ternary InGaAs/GaAs dot formation. Figure 3 shows the island concentrations as a function of deposition in Monolayers (ML) scale for conditions of high and low Arsine partial pressure. Curves (a) and (b) were obtained at low and high values of Arsine partial pressure. As can be seen, different values for critical thicknesses for the S-K transition are obtained. A higher critical thickness is obtained at high values of Arsine partial pressure, indicating that Arsine can act as a suppressant of the Stranski-Krastanow transformation. Similar growth suppression effects have been reported for InGaAs films, where 2-D growth could be maintained to higher depositions at lower temperatures [15] using molecular beam epitaxy. The result shown in figure 2 indicates that different values for 2-D to 3-D transition in III-V can be obtained depending on growth conditions. This result also shows that high Arsine values result in island formation at a slightly later stage, or for slightly higher film thicknesses.

Photoluminescence (PL) spectra of capped structures show that wetting layer (WL) PL energy does not shift beyond the onset of the S-K transition. Samples grown with a graded growth rate as in figure 3 (a) were capped, and PL measurements were done across 80 mm of varying InGaAs deposition. Luminescence emission begins with a thin QW which progressively red shifts (becomes thicker) as InGaAs deposition is increased. This is indicated in the lower portion of figure 4. In the next stage, the QD concentration rises until the threshold for QD PL detection. Once the QD PL peak increases in intensity, the WL peak diminishes rapidly. The evolution of WL to QD luminescence occurs over a broad range in QD concentrations but this

corresponds to a very narrow range in InGaAs deposition: from 4.08 ML to 4.14 ML. It can be seen from the spectra in figure 4 that PL emission intensities from QDs increases as their concentration increases, and that the WL emission is reduced. This is due to the growing dot concentration, and the inter-dot separation becoming smaller than photocarrier's diffusion lengths [17]. However, the energy of the weaker WL PL peak stays at the same value once the QD PL peak becomes detectable and the signal from QD related PL grows. These results indicate that the WL thickness does not increase (or decrease) with further InGaAs deposition once the QDs start forming. Slightly blue shifting (thinning or sacrificial) wetting layer emission has been observed under different growth conditions for InAs/GaAs dots [21].

In the next experiment, annealing of the InGaAs islands after formation was executed for 60 minutes, under the same Arsine partial pressures used during island growth and that produced the maximum island coverages indicated in figure 1. Another anneal was performed at high partial pressure (6×10^{-6}). The morphologies of the sample surfaces after such anneals are shown in Figure 5 (a, b, and c) for high Group V partial pressures and in 5 (d, e and f) for low arsine partial pressures. These are dramatic differences, since all other growth conditions such as temperature; impurities, Hydrogen flow, and growth rates were identical. As can be seen, coverages are lower and the size and density of large islands is higher than in 5 (d, e, f), which shows the results of a 60 minute anneal in 1×10^{-6} arsine partial pressure. The differences seem to indicate that significant ripening has occurred in the first case, while negligible ripening is seen in the other case. Several types of features can be seen from figures 5 (a) and 5 (b). The most prominent, and shown here in high resolution SEM imaging, are the large, dome shaped features. Vertical height measurements show these to be 10 times higher than the islands shown in 5 (d), 5(e) and 5 (f). As seen in 5 (c), these are faceted, with the same type of dome-like structure

reported for the growth of Si-Ge islands [9] and for TEM observation of in-situ ripening [7]. Other features were much flatter, and are shown in Figs 5 (a) and 5 (b) as faceted elongated hexagonal features and unformed large flat islands. No such structures were observed in the low AsH_3 growth. The observation of different types of islands indicates that the system was still under ripening after 1 hr anneal. Additional confirmation of the shape of these islands was obtained by cross sectional HRTEM [22]. An image of two buried InGaAs QDs is shown in figure 6. The same shape is observed for uncovered surface InGaAs dots and was confirmed by continuous tilting experiments along the [001] axis [23].

DISCUSSION

As seen in figure 1, large islands are not present at the highest coverage, indicating that coalescence is not favored under those conditions. At arsine flows above and below the amount for maximum island coverage, large islands were observed even though the deposition for the S-K transformation was not exceeded. This observation concurs with the observation of ripening at high arsine partial pressures, where the large domed islands shown are possibly the initial large islands ripened until all small islands were absorbed. The variation in average diameters for these large islands as a function of arsine partial pressures indicates the possibility that ripening and accelerated growth for incoherent islands is already occurring during sample cooling. Larger incoherent islands experience a higher rate of growth. Such accelerated growth rate for dislocated islands has been observed for Ge/Si islands [24] and explained [25] from differences in chemical potentials between differently strained islands. Such dissimilar rates of growth have the effect of enhancing the bimodal distribution in sizes. This effect is also observed here in InGaAs/GaAs island growth, and illustrated in figure 7, which shows islands grown under

similar AsH_3 PP as used for the islands shown in figure 2. Growth was stopped shortly after the S-K transformation in 7(a), and after an additional 2 ML deposition in 7(b).

Figure 1 shows that maximum island coverage is obtained with an "optimal" AsH_3 partial pressure. The island coverage rises to its maximum value at AsH_3 pp near 10^{-6}, and decreases for high values of AsH_3 pp. Different mechanisms might play a role on the island concentration shown on the right and left sides of the maximum value for coverage in figure 1. At very low group V pp, the possibility of group III reconstructed surfaces and their known effects on adatom mobilities must be considered.

We have shown that large variations in island density can be obtained with changes in the AsH_3 concentration, furthermore, dramatic differences are seen upon annealing. Our results also indicate that the conditions that promote low surface coverage also produce a later onset of the S-K transformation. These results also show that the conditions that promote low island densities produce metastable island configurations causing ripening even during cooling with no annealing. These differences in island coverage can be explained by considering the thermodynamic driving force in S-K island formation. In the formation of coherent S-K islands a reduction in strain energy is achieved at the expense of an increase in surface energy. The change in energy with formation of one island can be expressed as:

$$\Delta E_{isl} = \Delta E_{surf} + \Delta E_{ela}$$

where ΔE_{surf} is the cost in surface energy and ΔE_{ela} is the change in strain energy due to elastic relaxation. If the surface energy is lowered, islanding will be promoted for a fixed value of bulk elastic energy. Therefore, a decrease in island coverage suggests an increase in surface energy.

This leads to the surprising conclusion that Arsine can be used as an impurity free "surfactant". Impurities that raise surface energies were found in a study [14] showing different island shapes after prolonged annealing experiments with the addition of different surfactants impurities in Ge/Si island growth. It appears then that an "excess" AsH_3 during growth can act in an analogous manner in the growth of III-V compounds. Prolonged annealing under high AsH_3 pressures then decreases the island density and induces facetting. All experimental observations presented here are compatible with the attribution of a surfactant-like action of AsH_3 in high concentrations.

Ripening has been predicted for unstable or metastable configurations [26] with the implication that no ripening occurs if the system is in equilibrium. Therefore we believe that the arsine flows that produce the highest density of small islands can be used to achieve equilibrium growth of InGaAs islands on GaAs (100), since ripening is not observed even after prolonged annealing.

CONCLUSIONS

In conclusion, InGaAs/GaAs(100) island growth experiments done at different value of arsine partial pressure have shown that arsine can partially suppress the S-K transformation and drastically reduce island coverages. It was found that the same conditions that promote low island coverage also cause a later onset of the S-K transformation, resulting in thicker films before island formation is observed. We have also shown that it is possible to achieve thermodynamically stable smooth unfaceted island growth when surface energies are minimized in the growth of InGaAs by MOCVD.

ACKNOWLEDGEMENTS

The Authors acknowledge financial support from the Australian Research Council. Part of this work was started at the Australian National University, and was completed at the Jet Propulsion Laboratory, California Institute of Technology, under a contract with the National Aeronautics and Space Administration.

REFERENCES

1. D. J. Eaglesham and M. Cerrullo, Phys. Rev. Lett. **64**, 1943 (1990).

2. S. Guha, A. Maduhkar, and K. C. Rajkumar, Appl. Phys. Lett **57**, 2110 (1990).

3. C. W. Snyder, B. G. Orr, D. Kessler, and L. M. Sander, Phys. Rev. Lett. **66**, 3032 (1991).

4. D. Leonard, M. Krishnamurthy, C. M. Reaves, S. P. Denbaars, and P.M. Petroff, Appl. Phys. Lett **63**, 3203 (1993).

5. J. M. Moison, F. Houzay, F. Barthe, L. Leprince, E. Andre, and O. Vatel, Appl. Phys. Lett.**64**, 196 (1994).

6. R. Notzel, J. Temmyo, and T. Tamamura, Nature **369**, 131 (1994).

7. F. M. Ross, J. Tersoff, and R. M. Tromp, Phys. Rev. Lett. **80**, 984 (1998).

8. T. I. Kamins, E. C. Carr, R.S. Williams, and S. J. Rosner, J. Appl. Phys. **81**, 211 (1997).

9. G. Medeiros-Ribeiro, A. M. Bratkovski, T. I. Kamins, D. A. A. Ohlberg, and R. S. Williams, Science **279**, 353 (1998).

10. B. D. Min, Yong Kim, E. K. Kim, S-K Min, and M. J. Park, Phys. Rev. B **57**, 11879 (1998).

11. M. Copel, M. C. Reuter, E. Kaxiras, and R. M. Tromp, Phys. Rev. Lett. **63**, 632 (1989).

12. F. K. LeGoues, M. Copel and R. M. Tromp, Phys. Rev. Lett. **63**, 1826 (1989).

13. Y. Kumagai et al., Jpn. J. Appl. Phys. **35**, L476 (1996).

14. D. J. Eaglesham, F. C. Unterwald, and D. C. Jacobson, Phys. Rev. Lett. **70**, 966 (1993).

15. C. W. Snyder, J. F. Mansfield, and B. G. Orr, Phys. Rev. B **46**, 9551 (1992).

16. R. Leon, T. J. Senden, Yong Kim, C. Jagadish, and A. Clark, Phys. Rev. Lett **78**, 4942 (1997).

17. R. Leon and S. Fafard, Phys. Rev B 58, R1726 (1998).

18. R. Leon, C. Lobo, J. Zou, T. Romeo, and D. J. H. Cockayne, *Phys. Rev. Lett.* **81**, 2486 (1998).

19. D. Leonard, K. Pond and P. M. Petroff, Phys. Rev. B **50**, 11 687 (1994).

20. N. P. Kobayashi, T. R. Ramachandran, P. Chen, and A. Madhukar, Appl. Phys. Lett. **68**, 3299 (1996).

21. S. Fafard, Z. Wasilewski, C. Ni, D. Picard, M. Spanner, J. P. McCaffrey and P. G. Piva, to be published.

22. X. Z. Liao, J. Zou, X. F. Duan, D. J. H. Cockayne, R. Leon and C. Lobo, Phys. Rev B 58, R4235 (1998)

23. J. Zou, X. Z. Liao, D. J. H. Cockayne and R. Leon, Phys. Rev. B (in press).

24. M. Krishnamurthy, J. S. Drucker, and J. A. Venables, J. Appl. Phys. 69, 6461 (1991).

25. J. Drucker, *Phys. Rev. B* **48**, 203 (1993).

26. V. A. Shchukin, N. N. Ledentsov, P. S. Kop'ev, and D. Bimberg, Phys. Rev. Lett.**75**, 2968 (1995)

CAPTIONS

Figure 1. Variations in InGaAs island coverages as a function of AsH_3 partial pressure (pp). Growth at 550 °C for 5 ML deposition at a growth rate of 0.5 ML/sec. Solid diamonds show the variation in diameter for large (incoherent) islands. The fractional surface coverage is shown for small islands (hollow circles) and for large islands (solid circles).

Figure 2. [a] Plan view TEM micrograph (two beam) showing the morphology of the small and large InGaAs/GaAs [001] islands grown at high AsH_3 PP (6×10^6) without subsequent annealing or growth interruption. Micron bar is 100 nm. [b] Higher magnification on-zone bright-field image from same area.

Figure 3. Island concentrations as a function of coverage using conditions that produce a graded deposition. (a) at AsH_3 pp of 1.5×10^6, and (b) at AsH_3 pp of 6×10^6.

Figure 4. PL spectra and calibrated relative intensities in different regimes of QD formation. (a) WL PL shifts before QD formation, (b) evolution of PL spectra at low QD densities when both QD and WL peaks are simultaneously observed

Figure 5. (a), (b) FM images (deflection) and (c) high resolution SEM image of surface morphologies after 60 minutes anneals under high AsH_3 flows. (d), (e) FM images and (f) high resolution SEM micrograph of InGaAs islands annealed for 60 minutes under the same low AsH_3 flow that produces the maximum island densities shown in figure 1.

Figure 6. [110] cross-sectional HRTEM image of buried $In_{0.6}Ga_{0.4}As$ quantum dots showing two partially overlapping lens-shaped dots [22].

Figure 7. InGaAs/GaAs evolution in bimodal behavior for deposition beyond saturation island densities. Estimated deposition: a) 5.5 ML. b) 7.5 ML.

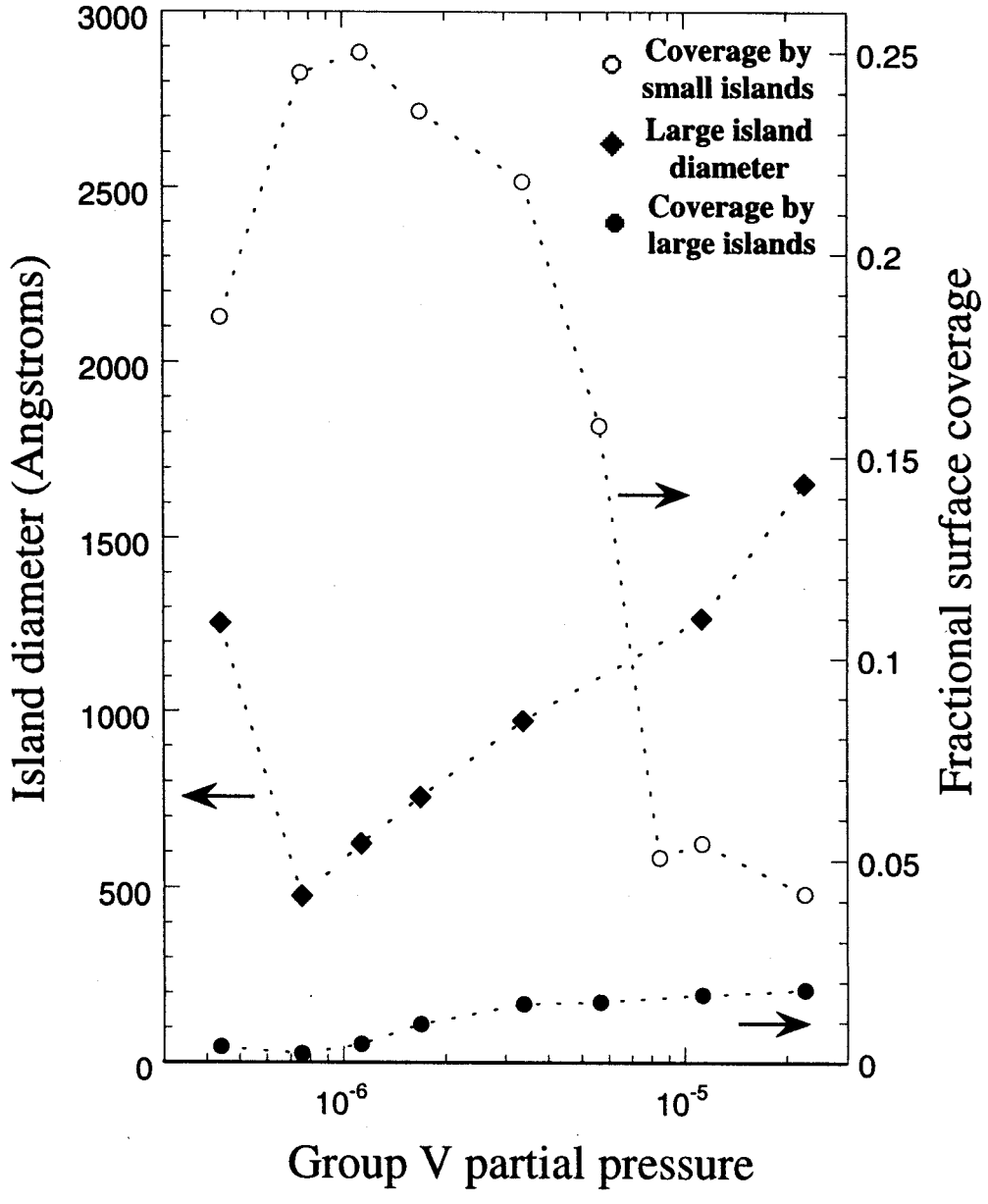
Coverage by small islands
Large island diameter
Coverage by large islands
Island diameter (Angstroms)
Fractional surface coverage
Group V partial pressure
3000
2500
2000
1500
1000
500
0
0.25
0.2
0.15
0.1
0.05
0
10^{-6}
10^{-5}

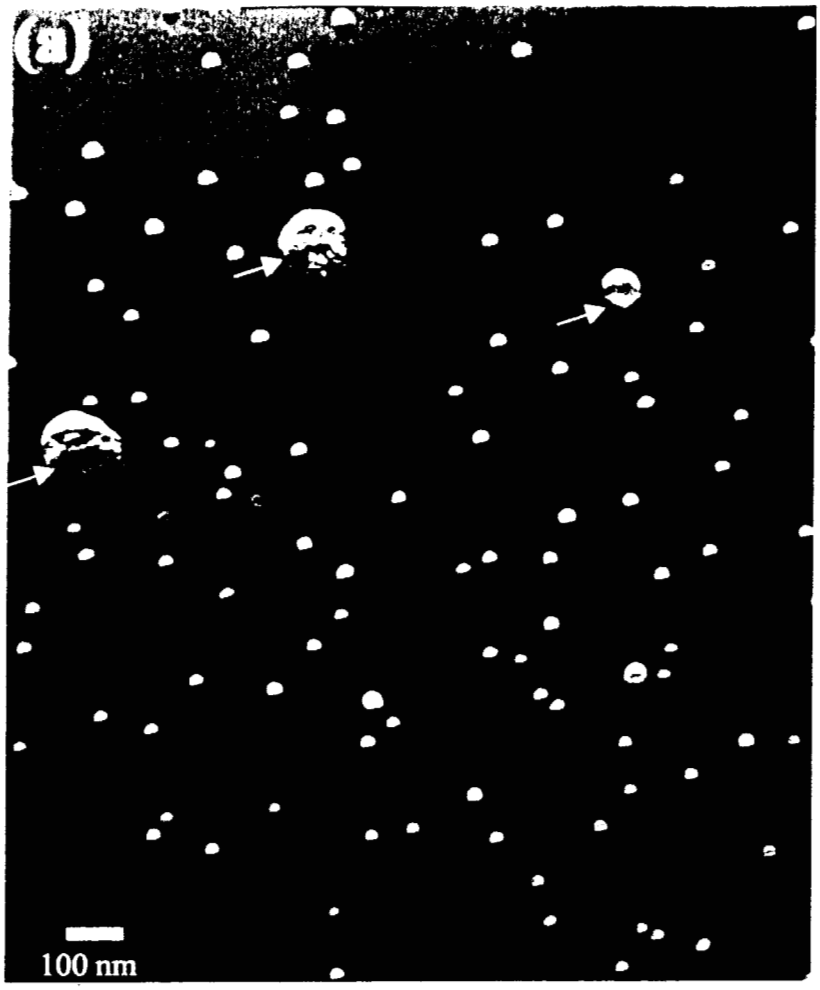
(a)
100 nm

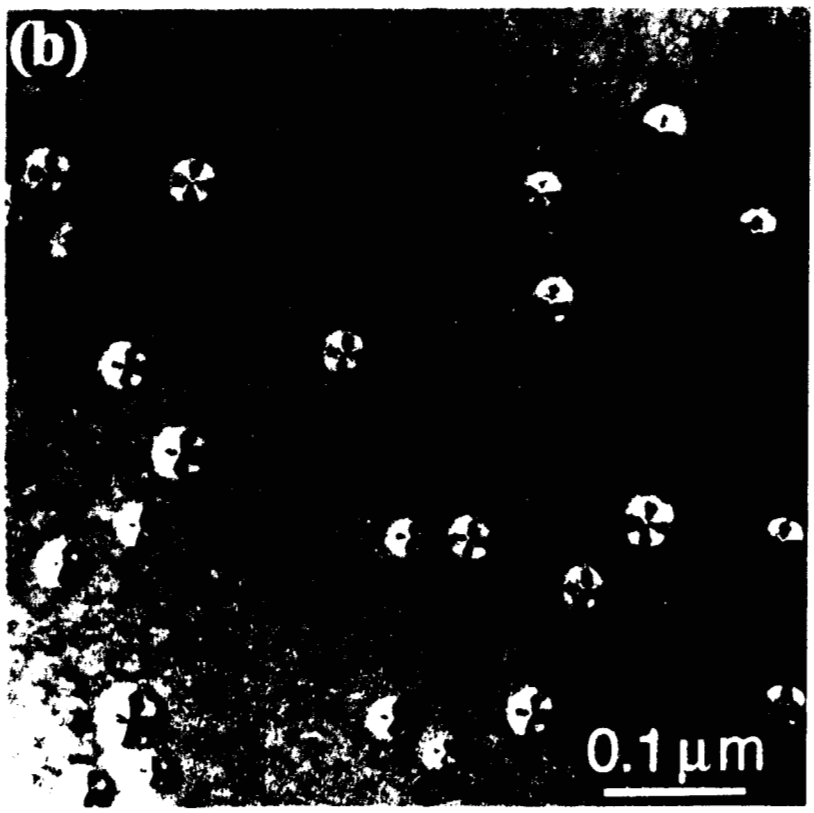
(b)
0.1 μm

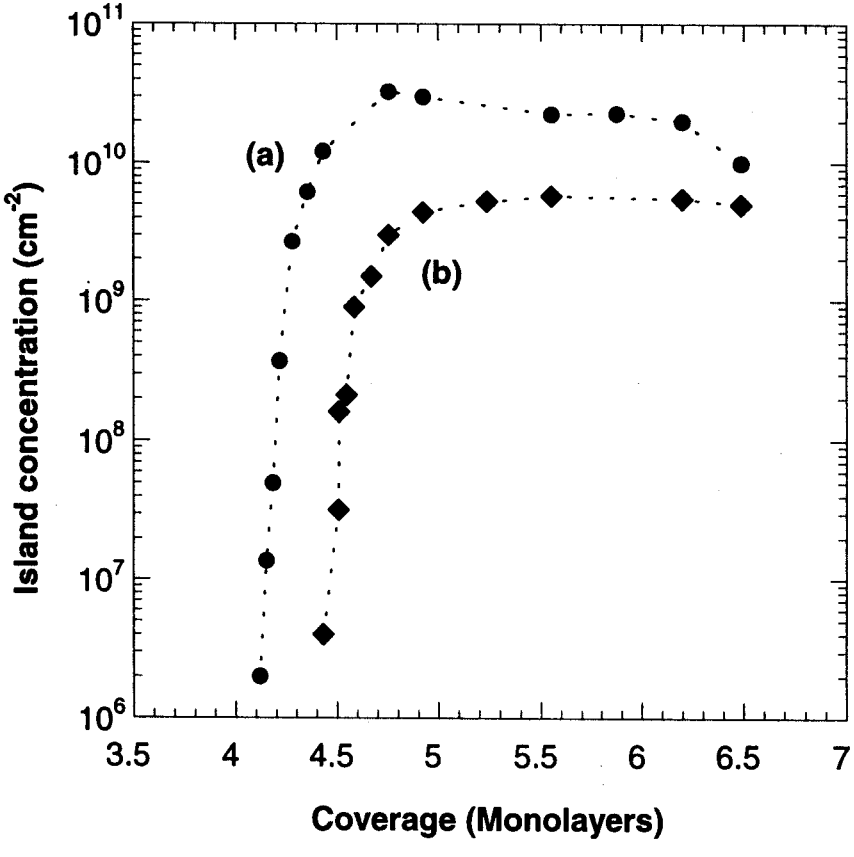
Island concentration (cm^{-2})
10^{11}
10^{10}
10^{9}
10^{8}
10^{7}
10^{6}
(a)
(b)
3.5
4
4.5
5
5.5
6
6.5
7
Coverage (Monolayers)

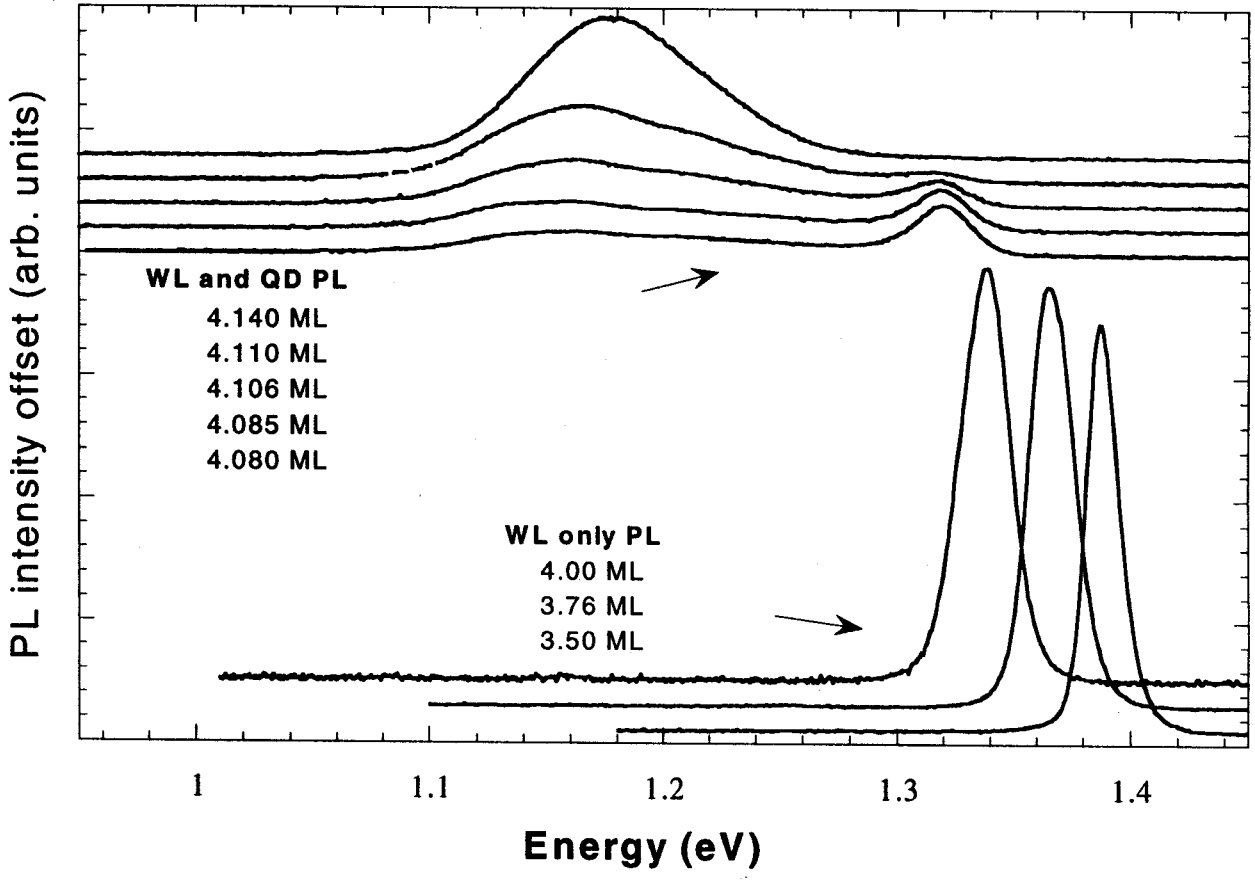
PL intensity offset (arb. units)
WL and QD PL
4.140 ML
4.110 ML
4.106 ML
4.085 ML
4.080 ML
WL only PL
4.00 ML
3.76 ML
3.50 ML
1
1.1
1.2
1.3
1.4
Energy (eV)

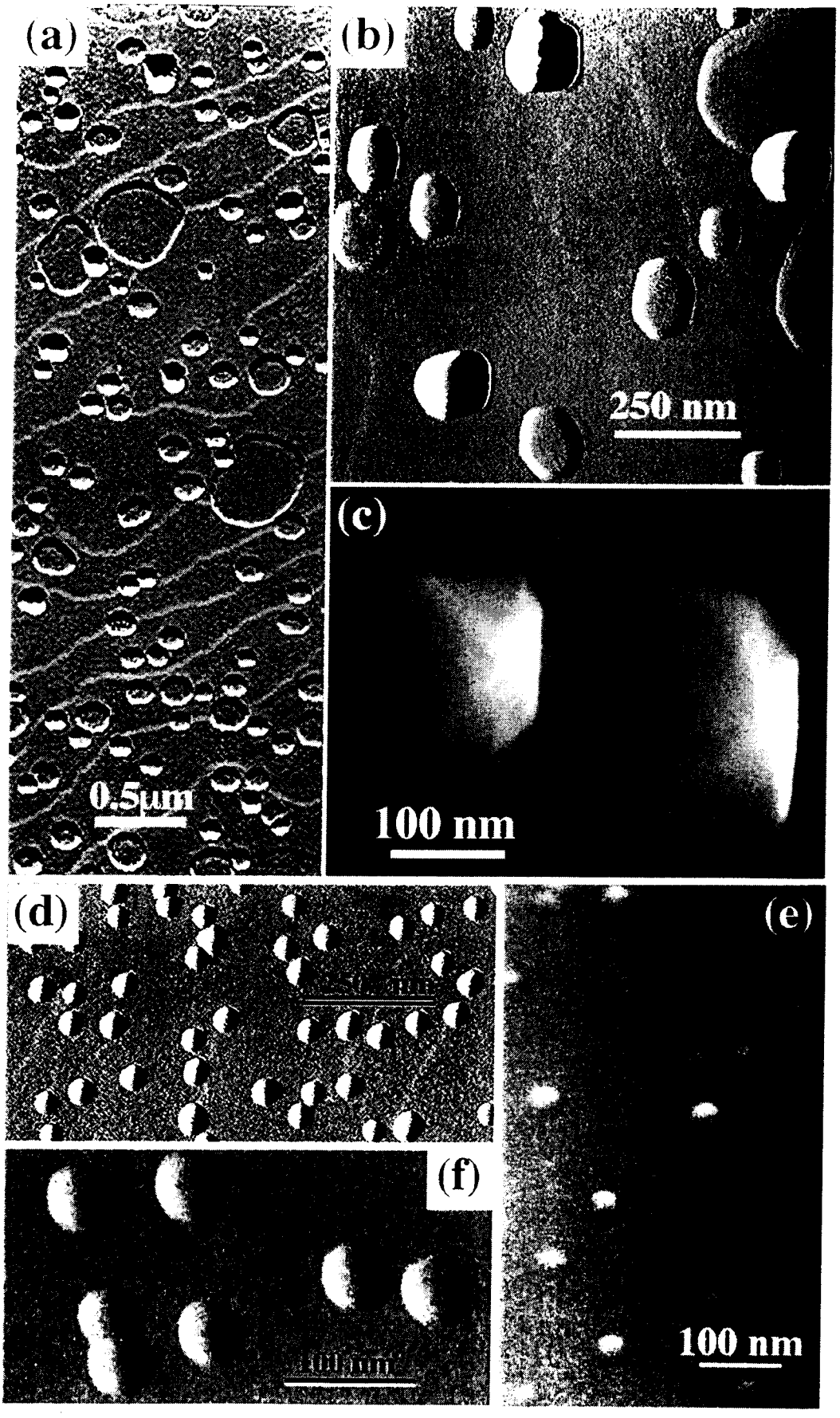
(a)
0.5μm
(b)
250 nm
(c)
100 nm
(d)
(e)
100 nm
(f)

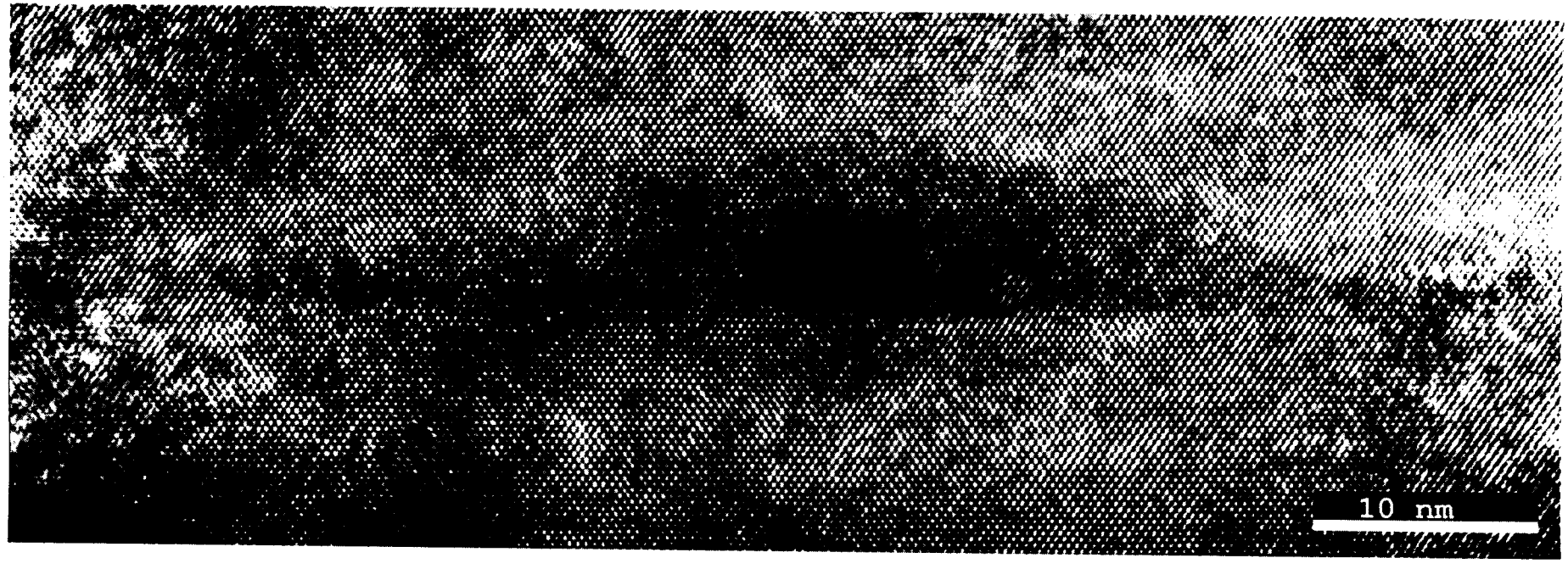
10 nm

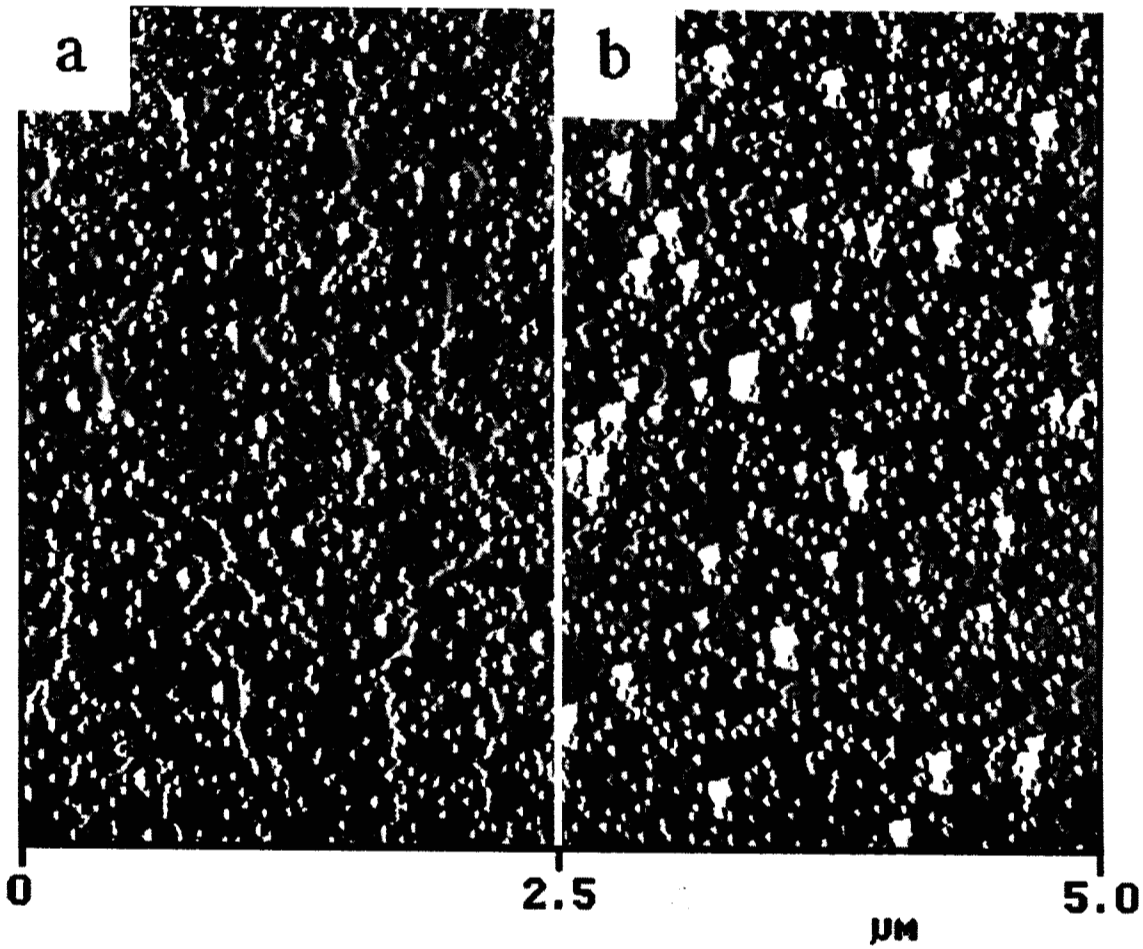
a
b
0
2.5
5.0
μM